Petr MACHNIK

VSB-Technical University of Ostrava

Analysis of EDCF Access Mechanism Based on IEEE 802.11e

Abstract. *This paper analyzes influence of the EDCF parameters on the performance of the IEEE 802.11 network. This aim is achieved using a mathematical model based on Markov chains. Furthermore, series of simulation results are demonstrated which are focused on the dependency of the throughput and media access delay on the load for distinct sets of EDCF parameters. By a similar way, DCF and EDCF access mechanisms are compared. Finally, an impact of the minimal and maximal contention window on the throughput and media access delay is examined.*

Streszczenie. *W artykule przedstawiono wpływ parametrów EDCF na działanie sieci IEEE 802.11. Wykorzystano do tego celu model matematyczny, oparty na łańcuchu Markova. Dodatkowo, wykonano serię symulacji, których wyniki pokazują zależność między przepustowością, a opóźnieniem w dostępie do danych przy różnych konfiguracjach parametrów EDCF. W podobny sposób dokonano porównania mechanizmów dostępu dla DCF oraz EDCF. Na koniec przedstawiono wyniki analizy wpływu rozmiarów (minimalnego i maksymalnego) okna rywalizacji na przepustowość i czas dostępu do danych.* ***(Analiza mechanizmu dostępu do danych EDCF, opartego na sieci IEEE 802.11e****).*

Keywords: EDCF, IEEE 802.11e, media access mechanism.
Słowa kluczowe: EDCF, IEEE 802.11e, mechanizm dostępu do danych.

Introduction

Initially, the IEEE 802.11 technology did not distinguish various types of data because, at that time, no delay-sensitive traffic was necessary to transmit by this wireless technology. Later, an accent was put on the Quality of Service (QoS) support so that delay-sensitive applications like voice or real-time video could be reliably transmitted. One of the solutions of this problem was an improvement of the used media access mechanism.

The original IEEE 802.11 standard defined two media access mechanisms – Distributed Coordination Function (DCF) and Point Coordination Function (PCF). Whereas DCF is a contention-based access mechanism similar to the CSMA/CD mechanism used by the Ethernet technology, PCF is a contention-free method. When PCF is employed, an access point polls stations that can transmit data. However, none of them supports the traffic differentiation.

In the year 2005, a novel standard IEEE 802.11e was published. One of the most important contributions of this standard is a definition of two new media access mechanisms called Enhanced Distributed Coordination Function (EDCF) and Hybrid Coordination Function (HCF). EDCF is an enhancement of DCF. HCF combines capabilities of both dissimilar mechanisms, EDCF and PCF.

In the most practical implementations of 802.11 networks, DCF or EDCF are used because of their simplicity and efficiency.

EDCF Parameters

The main contribution of EDCF in comparison with DCF is the use of four access categories. The principle of EDCF is very similar to DCF with the difference that access to the shared medium is influenced by many parameters, which are distinct for individual access categories. Fig. 1 illustrates the functioning of EDCF. Within EDCF, AIFS (Arbitration Interframe Space) is used as interframe space, which is at least as large as DIFS (DCF Interframe Space). The length of AIFS is different for different access categories. The longer is AIFS, the lower is the priority of frames.

The minimum value of the contention window CW_{min} can be also selected for each access category. CW_{min} is used to initialize the CW value. A random number between 0 and CW is chosen for each station as a back-off period otherwise two or more stations could start transmitting at the same moment after AIFS elapsing. The higher is CW_{min}, the lower is the priority of frames.

The CW_{max} value is the maximum possible value for CW on a per-category basis.

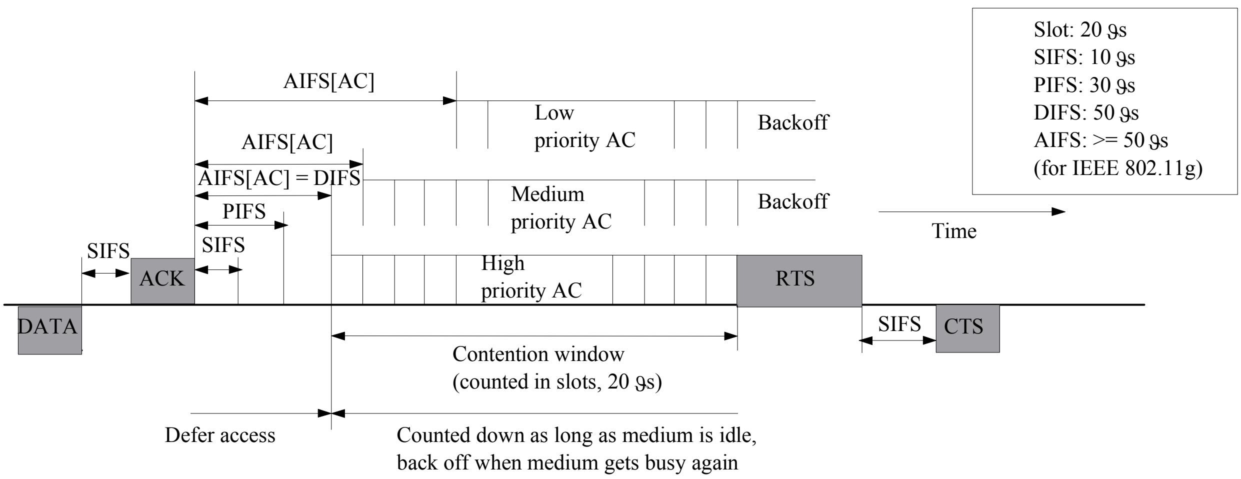

Fig.1. EDCF media access mechanism principle [2]

The fourth parameter dependent on the access category is the persistence factor (*PF*), which is used in case of an unsuccessful attempt to send data to calculate a new *CW* value according to the equation 1:

$$CW_{new}[AC] = ((CW_{old}[AC]+1)\cdot PF[AC]) - 1 \tag{1}$$

If the *PF* value equals 1 then the *CW* value does not change. If the *PF* value equals 2 then the new *CW* value is approximately twice the old *CW* (as well as in DCF). With increasing *PF*, the *CW* growth rate after each unsuccessful attempt to transmit data raises. The default value of *PF* is 2 for all access categories.

Within each station, four access categories have independent transmission queues. These queues behave as virtual stations with the described parameters determining their ability to transmit. A situation when two or more queues are trying to send their data simultaneously is called a virtual collision. The transmit opportunity (*TXOP*) is given to the category with the highest priority of the colliding access categories and the others back off as if a collision on the medium occurred.

More information about the EDCF mechanism can be found in [1, 2, 3].

Mathematical Model of EDCF Media Access Mechanism

The following mathematical model of the EDCF access mechanism is based on the models of the DCF and EDCF mechanism described in [4, 5, 6, 7, 8].

The most suitable tool to model the EDCF access method is a two-dimensional discrete-time Markov chain (see fig. 2).

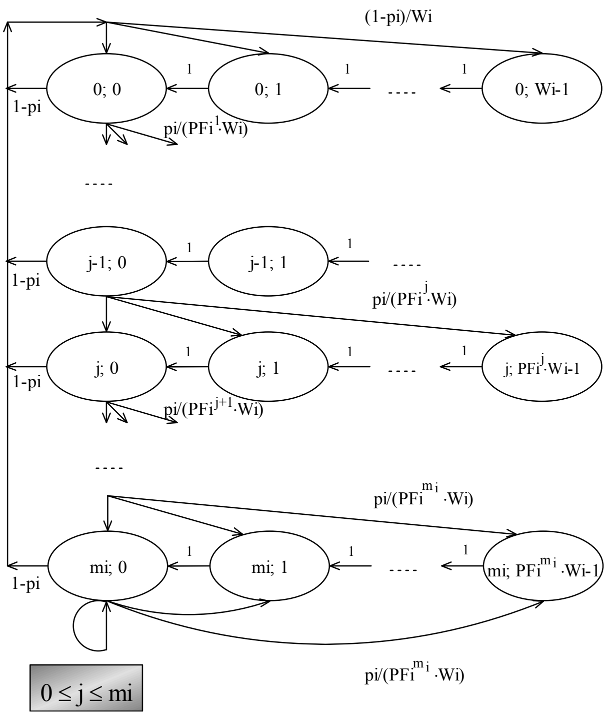

Fig.2. Scheme of an EDCF model by a two-dimensional discrete-time Markov chain

Let us assume that the channel conditions are ideal and that the system operates in saturation which means that a fixed number of stations always have a packet available for transmission.

Let N_i represents a number of traffic flows of a traffic type *i* (*i* = 1, 2, ..., *L*) belonging to an access category of a type *i*. *L* is a total number of access categories and is equal to 4 according to the IEEE 802.11e standard. Let $b_i(t)$ be the stochastic process representing the back-off time counter for a given access category of a type *i* that generates a pseudorandom number from the set $(0, 1, \ldots, CW_{min,i}-1)$. Moreover, let us define for convenience $W_i = CW_{\min,i}$ as the minimum contention window for an access category *i*. Then $CW_{\max,i} = PF_i^{m_i}\cdot W_i$ where m_i is the maximum back-off stage that leads to an increase of the contention window, i.e. until $CW \le CW_{max,i}$. Let $s_i(t)$ be the stochastic process representing the back-off stage $(0, 1, \ldots, m_i)$ for a given access category of a type *i*. Individual states in the two-dimensional discrete-time Markov chain are defined by couples of integers $\{s_i(t); b_i(t)\}$.

The main approximation in this model is that, at each transmission attempt for an access category of a type *i*, regardless of the number of retransmissions suffered, each packet collides with constant and independent probability p_i. This assumption is correct if values W_i and N_i are high.

Transition probabilities of this process are as follows:

$$\begin{aligned}
&P\{j,k \mid j,k+1\} = 1 \quad , \\
&\qquad j \in \{0,\ldots,m_i\},\quad k \in \{0,\ldots,PF_i^{j}\cdot W_i - 2\}, \\
&P\{0,k \mid j,0\} = \frac{1-p_i}{W_i} \quad , \\
&\qquad j \in \{0,\ldots,m_i\},\quad k \in \{0,\ldots,W_i - 1\}, \\
&P\{j,k \mid j-1,0\} = \frac{p_i}{PF_i^{j}\cdot W_i} \quad , \\
&\qquad j \in \{1,\ldots,m_i\},\quad k \in \{0,\ldots,PF_i^{j}\cdot W_i - 1\}, \\
&P\{m_i,k \mid m_i,0\} = \frac{p_i}{PF_i^{m_i}\cdot W_i} \quad , \quad k \in \{0,\ldots,PF_i^{m_i}\cdot W_i - 1\}
\end{aligned} \tag{2}$$

where it stands

$$P\{j_1,k_1 \mid j_0,k_0\} = P\left\{ \begin{matrix} s_i(t+1) = j_1, b_i(t+1) = k_1 \mid \\ \mid s_i(t) = j_0, b_i(t) = k_0 \end{matrix} \right\}. \tag{3}$$

Further, stationary distributions are described:

$$\begin{aligned}
&q_{j,0} = p_i^{j}\cdot q_{0,0} \quad , \quad j \in \{0,\ldots,m_i - 1\}, \\
&q_{m_i,0} = \frac{p_i^{m_i}}{1-p_i}\cdot q_{0,0}, \\
&\qquad \text{because}\; q_{m_i,0} = p_i\cdot q_{m_i,0} + p_i\cdot q_{m_i-1,0}, \\
&q_{j,k} = \frac{PF_i^{j}\cdot W_i - k}{PF_i^{j}\cdot W_i}\cdot q_{j,0} \quad , \quad k \in \{0,\ldots,PF_i^{j}\cdot W_i - 1\}, \\
&\text{where}\; q_{j,k} = \lim_{t\to\infty} P\{s_i(t) = j, b_i(t) = k\}.
\end{aligned} \tag{4}$$

The value of $q_{0,0}$ can be derived by this way:

$$\begin{aligned}
&1 = \sum_{j=0}^{m_i}\sum_{k=0}^{PF_i^{j}\cdot W_i - 1} q_{j,k} \quad , \quad m_i \in \{0,1,\ldots\},\; W_i \in \{1,2,\ldots\}, \\
&1 = \sum_{j=0}^{m_i}\left(q_{j,0}\cdot \sum_{k=0}^{PF_i^{j}\cdot W_i - 1} \frac{PF_i^{j}\cdot W_i - k}{PF_i^{j}\cdot W_i} \right) \quad , \quad W_i \ge 1, \\
&\text{for each } j \text{ such as } 0 \le j \le m_i, m_i \ge 0, \text{ it stands}
\end{aligned} \tag{5}$$

(by using an expression for a sum of arithmetic progression items)

$$
1=\sum_{j=0}^{m_i} q_{j,0}\cdot\frac{\left(PF_i^{\,j}\cdot W_i+1\right)}{2},
$$

(6)
$$
1=\sum_{j=0}^{m_i-1}\left[q_{0,0}\cdot p_i^{\,j}\cdot\frac{\left(PF_i^{\,j}\cdot W_i+1\right)}{2}\right]
+q_{0,0}\frac{p_i^{m_i}}{1-p_i}\cdot\frac{\left(PF_i^{m_i}\cdot W_i+1\right)}{2},
$$

$$
\text{and because of } \sum_{j=0}^{m_i} q_{j,0}=\frac{q_{0,0}}{1-p_i},
$$

$$
1=\frac{q_{0,0}}{2}\cdot\left[W_i\cdot\left(\sum_{j=0}^{m_i-1}\left(PF_i\cdot p_i\right)^j+\frac{\left(PF_i\cdot p_i\right)^{m_i}}{1-p_i}\right)+\frac{1}{1-p_i}\right],
$$

(by using an expression for the sum of geometric progression items and L'Hospital rule)

(7)
$$
q_{0,0}=\begin{cases}\dfrac{2\cdot(1-p_i)}{W_i(1-p_i)m_i\left(PF_i\cdot p_i\right)^{m_i-1}+W_i\left(PF_i\cdot p_i\right)^{m_i}+1}, & p_i=\dfrac{1}{PF_i},\\[2ex] \dfrac{2\cdot(1-p_i)}{W_i(1-p_i)\dfrac{1-\left(PF_i\cdot p_i\right)^{m_i}}{1-PF_i\cdot p_i}+W_i\left(PF_i\cdot p_i\right)^{m_i}+1}, & p_i\neq\dfrac{1}{PF_i}.\end{cases}
$$

The probability τ_i that a back-off entity of a type i is transmitting in a generic slot time is calculated by the summation of all stationary distributions $q_{j,0}$.

(8)
$$
\tau_i=\sum_{j=0}^{m_i} q_{j,0}=\frac{q_{0,0}}{1-p_i}=
=\frac{2\cdot(1-PF_i\cdot p_i)}{W_i(1-p_i)\left[\,1-\left(PF_i\cdot p_i\right)^{m_i}\,\right]+W_i\left(PF_i\cdot p_i\right)^{m_i}\left(1-PF_i\cdot p_i\right)+1-PF_i\cdot p_i}
$$

The probability of a collision can be expressed as:

(9)
$$
p_i=1-\left(1-\tau_i\right)^{N_i-1}\prod_{h=1,h\neq i}^{L}(1-\tau_h)^{N_h}.
$$

Values of τ_i and p_i can be numerically calculated from two previous equations.

Following probabilities and duration times can be derived by using previous calculations:

(10)
$$
P_{idle}=\prod_{i=1}^{L}\left(1-\tau_i\right)^{N_i},
$$
$$
P_{busy}=1-P_{idle}=1-\prod_{i=1}^{L}\left(1-\tau_i\right)^{N_i},
$$
$$
P_{success,i}=\begin{cases}0, & P_{busy}=0,\\ \dfrac{1}{P_{busy}}\cdot N_i\cdot\tau_i\cdot\left(1-\tau_i\right)^{N_i-1}\cdot\prod\limits_{h=1,h\neq i}^{L}\left(1-\tau_h\right)^{N_h}, & P_{busy}\neq 0,\end{cases}
$$
$$
P_{collision,i}=1-P_{success,i},
$$

where P_{idle} is probability that the transmission medium is idle,

P_{busy} is probability that the transmission medium is busy,

$P_{success,i}$ is probability that the transmission attempt of a category i is successful,

$P_{collision,i}$ is probability that the transmission attempt of a category i is unsuccessful.

T_{idle} - *slot time* (It depends on the type of the physical layer.)

(11)
$$
T_{success,i}=\begin{cases}T_{PLCP}+\delta+T_{SIFS}+T_{ACK}+\delta+\\ +T_{AIFS,i}\quad(\text{without RTS/CTS}),\\ (T_{RTS}+\delta+T_{SIFS}+T_{CTS}+\delta+T_{SIFS})+\\ +T_{PLCP}+\delta+T_{SIFS}+T_{ACK}+\delta+T_{AIFS,i}\\ (\text{with RTS/CTS}).\end{cases}
$$
$$
T_{collision,i}=\begin{cases}T_{PLCP}+\delta+T_{AIFS,i}\ (\text{ without RTS/CTS}),\\ T_{RTS}+\delta+T_{AIFS,i}\quad(\text{with RTS/CTS}).\end{cases}
$$

where T_{idle} is a period when the transmission medium is idle,

$T_{success,i}$ is a period of an successful transmission of a category i,

$T_{collision,i}$ is a period of an unsuccessful transmission of a category i,

T_{PLCP}, T_{RTS}, T_{CTS} represent periods that are necessary to send a PLCP, RTS, CTS frame respectively,

T_{AIFS}, T_{SIFS} represent corresponding interframe spaces,

T_{data} represents a period used for transmitting MAC sublayer payload,

δ is a propagation delay.

Finally, we can express normalized saturation throughput for the EDCF media access mechanism:

(12)
$$
S=\sum_{i=1}^{L}S_i=
=\frac{P_{busy}\cdot\sum\limits_{i=1}^{L}P_{success,i}\cdot T_{data}}{P_{busy}\cdot\sum\limits_{i=1}^{L}\left(P_{success,i}\cdot T_{success,i}\right)+P_{busy}\cdot\sum\limits_{i=1}^{L}\left(P_{collision,i}\cdot T_{collision,i}\right)+P_{idle}\cdot T_{idle}}.
$$
$$
S\in(0;1).
$$

The saturation is normalized with regard to the physical layer technology. The higher is the saturation throughput the more effective is time spent for transmitting of useful data compared with time spent because of an overhead, a collision recovery and a back-off delay. Probabilities in the equation serve as influence weights of time items on the throughput.

Further, we will analyze the equation 12 more in detail. Let us proceed with the equation 9:

$$
p_i=1-\left(1-\tau_i\right)^{N_i-1}\prod_{h=1,h\neq i}^{L}(1-\tau_h)^{N_h},
$$
$$
1-p_i=\frac{\prod\limits_{i=1}^{L}(1-\tau_i)^{N_i}}{1-\tau_i},
$$

(13)
$$
\left(1-p_{i1}\right)\left(1-\tau_{i1}\right)=\left(1-p_{i2}\right)\left(1-\tau_{i2}\right)=\prod_{i=1}^{L}(1-\tau_i)^{N_i},
$$
$$
1\leq i,i1,i2\leq L,
$$

where i1 and i2 are indexes for two different access categories. If $\tau_{i1}\neq\tau_{i2}$ then $p_{i1}\neq p_{i2}$.

From the equation 8, it follows that if $W_{i1} >> 1$ and $W_{i2} >> 1$ then $\tau_{i1} << 1$ and $\tau_{i2} << 1$. Based on these assumptions, we can conclude for the equation 13 that $p_{i1} \approx p_{i2}$. Next, if $W_{i1} >> 1$, $W_{i2} >> 1$, $m_{i1} \approx m_{i2}$ and $PF_{i1} \approx PF_{i2}$, the equation 8 can be simplified to the form described in the equation 14.

$$(14) \qquad \frac{\tau_{i1}}{\tau_{i2}} \approx \frac{W_{i2}}{W_{i1}}$$

From the equation 12 and using the equation 10, it is possible to derive:

$$\frac{S_{i1}}{S_{i2}} = \frac{P_{success,i1} \cdot T_{data,i1}}{P_{success,i2} \cdot T_{data,i2}} = \frac{N_{i1} \cdot \tau_{i1} \cdot (1-\tau_{i2}) \cdot T_{data,i1}}{N_{i2} \cdot \tau_{i2} \cdot (1-\tau_{i1}) \cdot T_{data,i2}} \approx$$

$$\approx \frac{N_{i1} \cdot \tau_{i1} \cdot T_{data,i1}}{N_{i2} \cdot \tau_{i2} \cdot T_{data,i2}} \approx \frac{N_{i1} \cdot W_{i2} \cdot T_{data,i1}}{N_{i2} \cdot W_{i1} \cdot T_{data,i2}}$$

$$(15) \qquad \frac{S_{i1}}{S_{i2}} \approx \frac{\dfrac{N_{i1} \cdot T_{data,i1}}{W_{i1}}}{\dfrac{N_{i2} \cdot T_{data,i2}}{W_{i2}}}$$

Previous considerations proceed from many simplifying assumptions, nevertheless, it is quite accurate to state that a ratio between two normalized saturation throughputs of different access categories is firstly given by values of CW_{min} and T_{data} of individual access categories. We assume that *N* is constant in a given event. With the growing number of collisions in the network, the influence of parameters CW_{max} and PF increases.

By the similar way, a ratio between two media access delays $T_{MAD,i}$ of different access categories can be calculated. We assume that $N_{i1} >> 1$ and $N_{i2} >> 1$.

$$(16) \qquad \frac{T_{MAD,i1}}{T_{MAD,i2}} \approx \frac{W_{i1}}{W_{i2}}$$

According to this formula, we can state that a ratio between two media access delays is mainly influenced by a ratio of CW_{min} values of the corresponding access categories.

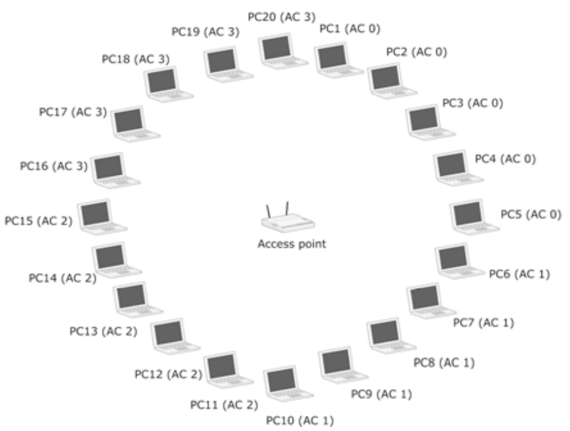

Fig.3. Network topology for simulations

Simulation Results

All simulations were made by the OPNET Modeler network simulation program. The simulated network topology consisted of 20 stations and one access point (see fig. 3). The distance of stations from the access point was about 20 meters without any obstacles. The IEEE 802.11g technology was used at the physical layer. All devices supported the EDCF mechanism and traffic differentiation. Wireless stations were divided equally for five among four groups. Each group generated traffic belonging to one of access categories. The length of packets created by stations was 1000 bytes. Packets were generated by stations with the constant probability. Their interarrival time was changed to influence the offered load. Three sets of EDCF parameters for individual access categories were used to demonstrate their influence on the data throughput and media access delay. Their values are shown in tables 1 – 3. The RTS/CTS mechanism was not used in these simulations.

Table 1. EDCF parameters set no. 1
(recommended and usually default values)

Access Category	EDCF Parameters			
	CW_{min}	*CW_{max}*	*AIFS[µs]*	*TXOP[ms]*
0	15	1023	150	0
1	15	1023	70	0
2	7	15	50	3
3	3	7	50	1.5

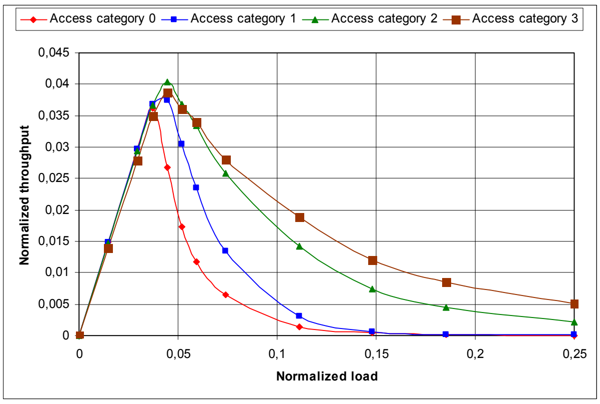

Fig.4. Graph for comparison of EDCF access categories (set no. 1)

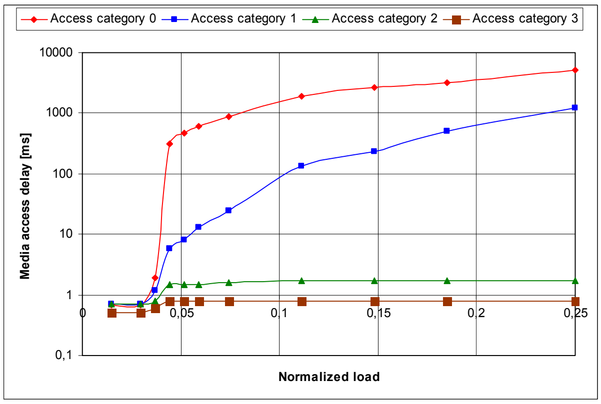

Fig.5. Graph for comparison of EDCF access categories (set no. 1)

Results of the first set of simulations arise from the graphs in fig. 4 and 5. The first graph describes the dependency of the throughput on the load for individual access categories. A peak of the throughput is possible to see herein. Further growth of the load induces more collisions and thereby lower throughput. The second graph shows the dependency of the media access delay on the load for individual access categories. The load and throughput are analyzed from a perspective of the MAC sublayer and are normalized with regard to the theoretical bit rate at the physical layer (54 Mbps for IEEE 802.11g).

In the second set of simulations, EDCF parameters with very close values were used (see table 2). As a result, throughput values for individual access categories are nearly the same (see fig. 6). The media access delay for low priority access categories is lower compared with the previous simulations (see fig. 7).

Table 2. EDCF parameters set no. 2

Access Category	EDCF Parameters			
	CW_{min}	CW_{max}	*AIFS[μs]*	*TXOP[ms]*
0	15	127	50	0
1	7	127	50	0
2	3	15	50	3
3	3	7	50	1.5

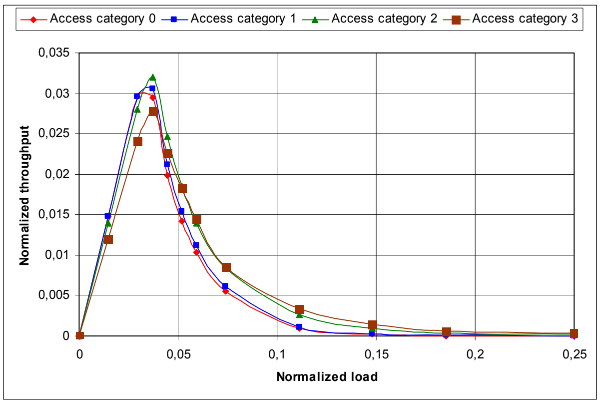

Fig.6. Graph for comparison of EDCF access categories (set no. 2)

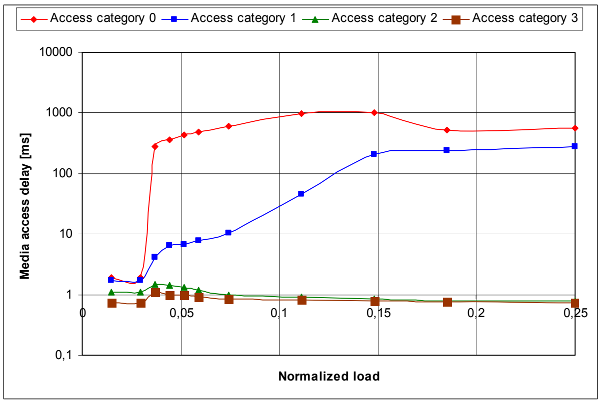

Fig.7. Graph for comparison of EDCF access categories (set no. 2)

Table 3. EDCF parameters set no. 3

Access Category	EDCF Parameters			
	CW_{min}	CW_{max}	*AIFS[μs]*	*TXOP[ms]*
0	127	4095	210	0
1	31	1023	90	0
2	3	15	50	3
3	1	7	50	1.5

The third set of simulations demonstrates the effect of very dissimilar values of EDCF parameters (see table 3). As can be seen in fig. 8, only access categories 2 and 3 can be effectively used to transport data during the high throughput. Within access categories 0 and 1, the data throughput is very low. The media access delay (see fig. 9) is quite high within all access categories compared with results of other simulations because of high EDCF parameters within categories 0 and 1 and many collisions of frames within categories 2 and 3 that have close values of EDCF parameters.

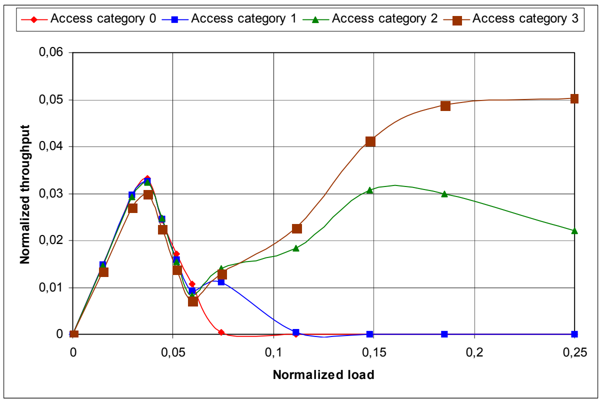

Fig.8. Graph for comparison of EDCF access categories (set no. 3)

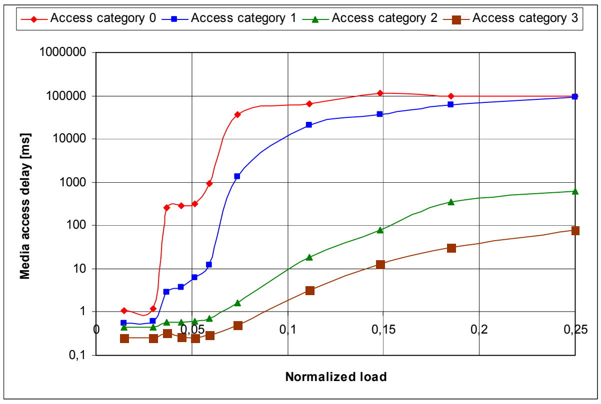

Fig.9. Graph for comparison of EDCF access categories (set no. 3)

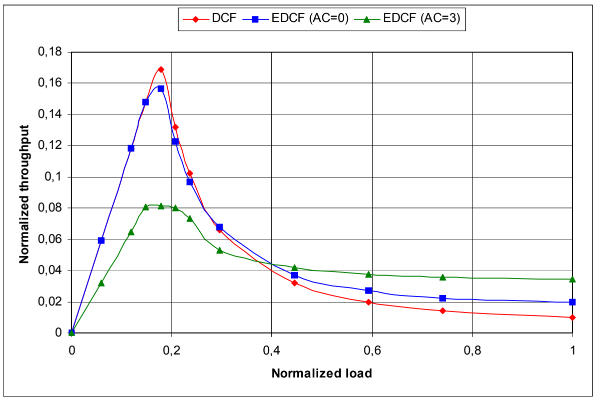

Fig.10. Graph for comparison of DCF and EDCF

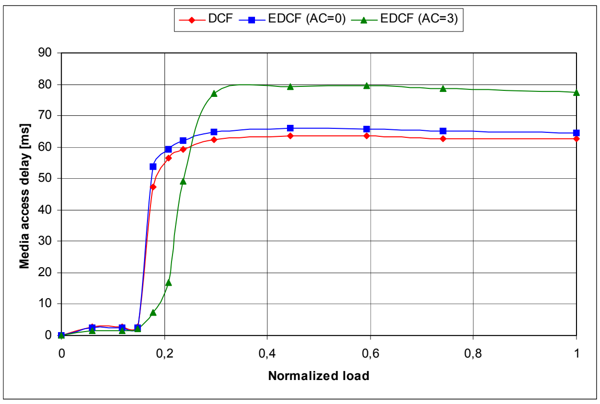

Fig.11. Graph for comparison of DCF and EDCF

Further two graphs in fig. 10 and 11 compare performance of the simulated network which successively used DCF access mechanism, the EDCF access mechanism if all traffic belongs to the least priority access category 0, and EDCF access mechanism if all traffic belongs to the most priority access category 3. For EDCF simulations, the default values of EDCF parameters were applied (see table 1).

As can be seen in the graphs, DCF and EDCF (access category 0) show similar results because they have similar values of media access mechanism parameters. EDCF (access category 3) has worse results of the throughput during a lower load. The reason is lower CW values which lead to frequent collisions if all traffic is marked only with this high priority. During a higher load, the number of collisions is high in all cases.

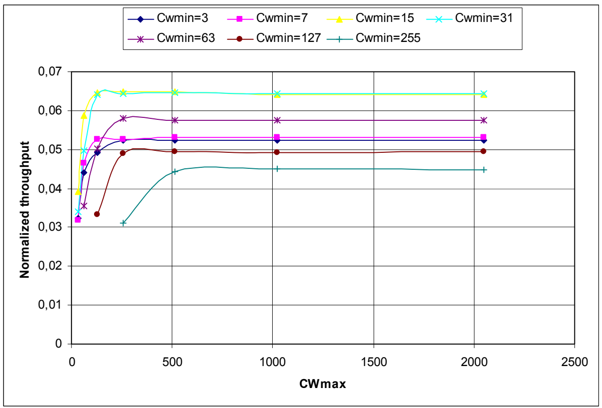

Fig.12. Graph that illustrates influence of CW_{min} and CW_{max} on throughput

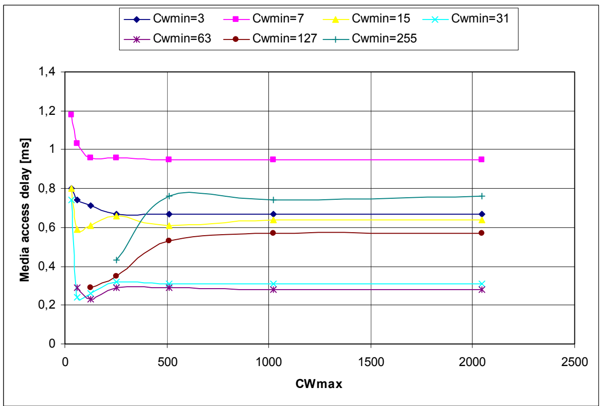

Fig.13. Graph that illustrates the influence of CW_{min} and CW_{max} on media access delay

In fig. 12 and 13, graphs are shown that illustrate the influence of the minimal and maximal contention window on the normalized throughput and media access delay. It is obvious that a strong influence of CW_{min} parameter but a small influence of CW_{max} parameter exist. However, if both parameters have close values then the throughput is low and the delay is high. Best results from all simulations (high throughput and low media access delay) were accomplished when CW_{min} = 31 and CW_{max} =127 (or higher). Simulations were performed with a traffic load 12.8 Mbps.

Conclusion

In this paper, IEEE 802.11e EDCF media access mechanism was described. It was illustratively shown how its parameters – CW_{min}, CW_{max}, AIFS, and PF – influence performance of the network which uses this access mechanism. The mathematical analysis of the EDCF media access mechanism was based on Markov chains. A formula for the normalized saturation throughput was derived thereby the influence of EDCF parameters was illustrated. Further, simplified formulas for the throughput and media access delay were derived. Realized simulations demonstrated the dependency of the throughput and media access delay on the load for distinct access categories and for three sets of EDCF parameters. A significant difference among individual access categories was found out. The priority of traffic belonging to a specific access category is strongly affected by the used EDCF parameters values. Furthermore, similar simulations were carried out to compare the DCF and EDCF mechanism. The created graphs indicate that the high priority access category works poorly if all traffic belongs to it. Finally, a dominant influence of the CW_{min} parameter on the throughput and media access delay was shown.

The research leading to these results has received funding from the European Community's Seventh Framework Programme (FP7/2007-2013) under grant agreement n° 218086.

REFERENCES

[1] *IEEE 802.11e Standard : Wireless LAN Medium Access Control (MAC) and Physical Layer (PHY) specification - Medium Access Control Quality of Service Enhancements* [online]. 2005. Available: http://standards.ieee.org/getieee802/download/802.11e-2005.pdf.
[2] Ohrtman F., *Voice over 802.11.* Boston: Artech House, 2004, 258 p. ISBN 1580536778.
[3] Roshan P., Leary J., *Wireless Local Area Network Fundamentals.* Cisco Press, 2003, 300 p. ISBN 1587050773.
[4] Machnik, P., Analysis of IEEE 802.11e EDCF Media Access Mechanism. In *Proceedings of the 11th International Conference Knowledge in Telecommunication Technologies and Optics KTTO 2011*. Ostrava: VSB-Technical University of Ostrava, 2011. ISBN 978-80-248-2399-7.
[5] Machnik, P., Mathematical Modeling and Simulation of EDCF Media Access Mechanism in IEEE 802.11 Technology. In *Proceedings 31th International Conference Telecommunications and Signal Processing 2008*. Budapest: Asszisztencia Szervező Kft., 2008. ISBN 978-963-06-5487-6.
[6] Bianchi G., Performance Analysis of the IEEE 802.11 Distributed Coordination Function. In *Selected Areas in Communications, IEEE Journal*. 2000, pp. 535-547. ISSN 0733-8716.
[7] Li B., Battiti R., Performance Analysis of An Enhanced IEEE 802.11 Distributed Coordination Function Supporting Service Differentiation. In *Quality for All : 4th COST 263 International Workshop on Quality of Future Internet Services, QoFIS 2003*. Berlin: Springer, 2003, pp. 152-161. ISBN 9783540201922.
[8] Mangold S., Analysis of IEEE 802.11e and Application of Game Models for Support of Quality-of-Service in Coexisting Wireless Networks. Mainz : Wissenschaftsverlag Mainz, 2003. 269 p. ISBN 3860739850.

***Author**: Petr Machnik, VSB-Technical University of Ostrava, Department of Telecommunications, 17. listopadu 15, 70833 Ostrava, E-mail: petr.machnik@vsb.cz.*